Doctoral Dissertation

Low Temperature-Operative Carbon Monoxide Gas Sensors Employing Novel Catalysts Based on Oxides with Rare Earths

（希土類複合酸化物系触媒を用いた低温作動型一酸化炭素ガスセンサ）

Ayaka Hosoya

January 2017

Department of Applied Chemistry
Graduate School of Engineering
Osaka University

Low Temperature-Operative Carbon Monoxide Gas Sensors Employing Novel Catalysts Based on Oxides with Rare Earths

（希土類複合酸化物系触媒を用いた低温作動型一酸化炭素ガスセンサ）

2017

Ayaka Hosoya

Department of Applied Chemistry
Graduate School of Engineering
Osaka University

Preface

The work of this thesis has been carried out under the supervision of Professor Dr. Nobuhito Imanaka at Department of Applied Chemistry, Graduate School of Engineering, Osaka University.

The object of this thesis is to develop the catalytic combustion-type carbon monoxide gas sensor which is operable at relatively low temperatures.

The author wishes that the findings and the knowledge obtained in this work will provide useful suggestions and information for further development and design of low temperature-operative catalytic combustion-type gas sensors.

Ayaka Hosoya

Department of Applied Chemistry

Graduate School of Engineering

Osaka University

2-1 Yamadaoka, Suita,

Osaka 565-0871,

Japan

January 2017

Contents

Chapter 3

Catalytic combustion-type CO gas sensor with Pt-free catalyst

General Introduction

Carbon monoxide (CO) is a well-known highly toxic gas causing serious health damages on human body even at low concentration due to the 250 times higher binding ability of CO molecule to hemoglobin than that of O_2. CO is generated not only in industrial activities but also in our daily lives by such incomplete combustion of stoves, which causes tragic CO poisoning accidents every year. Since CO is colorless and odorless gas, we cannot sense the generation of CO in ambient atmosphere and we always need to use some equipment to detect CO gas. For the rapid detection of CO generation, it is essential to put the compact and inexpensive CO gas sensors at every sites with the potential for CO gas generation.

Until now, various kinds of compact CO gas monitoring devices have been developed such as those based on semiconductor [1-6], potentiostat [7-10] and catalytic combustion [11-14]. Semiconductor-type CO gas sensor detects the CO gas concentration as the electrical resistance change of the semiconductor, which is originated by CO gas adsorption on the semiconductor surface. Although the semiconductor-type sensor can exhibit stable performance owing to its simple sensor construction and a sensing mechanism, this type of sensor basically has a drawback in that several kinds of gases other than CO can adsorb on the semiconductor surface and produce sensor signals, meaning that the selectivity of this type of sensor is inherently low. Potentiostat-type CO gas sensor exhibits selective CO gas detection by the operation at which appropriate voltage for CO oxidation is applied to the sensor, but it cannot operate over prolonged period of time because the liquid electrolyte used in the device eventually evaporates. On the other hand, catalytic combustion-type CO gas sensor is established by a simple detection system consisting of only Pt coil combined with a CO oxidation catalyst, and is capable of stable and rapid sensing performance over long periods of time, similar to the semiconductor-type sensors. While catalytic

combustion-type sensor also detects CO gas by the resistance change of the Pt coil, its resistance change is resulted from the heat generated by the combustion of CO gas on the catalyst loaded over the Pt coil. Therefore, the resistance change of Pt coil is theoretically controlled by the application of catalyst which can selectively oxidize CO. However, there is a major problem for the conventional catalytic combustion-type CO gas sensor, that is, the conventional catalysts of Pt/Al_2O_3 or Pd/Al_2O_3 required several hundred Celsius degrees (ca. 400 °C) for complete CO oxidation. At such elevated temperatures, other flammable gases such as volatile organic compounds (formaldehyde, toluene, etc.) are always oxidized, and the sensors with conventional catalysts could not show selectivity for CO gas. To solve this problem, it is necessary to develop the novel CO oxidation catalysts that can oxidize CO gas at considerably lower temperatures at which other gases are not oxidized.

In the previous studies on environmental remediation catalysts conducted at by the laboratory I belong, the Pt-loaded CeO_2–ZrO_2–MO_x solid solution (M = Sn, Zn) supported γ-Al_2O_3 have been reported to show high catalytic activities for the oxidation of VOCs [15-18] even at lower temperatures than other corresponding catalysts. For the VOCs oxidation by the Pt-loaded CeO_2–ZrO_2–MO_x solid solution supported γ-Al_2O_3, their high catalytic activities were considered to emerge by the acceleration of oxide anion conduction in the CeO_2–ZrO_2–MO_x solid solution which is realized by the generation of intentional oxide anion vacancy in the structure.

Based on the above described background, I focused on the Pt-loaded CeO_2–ZrO_2–MO_x solid solution as a novel CO oxidation catalyst which is applicable to the catalytic combustion-type CO gas sensor operable at considerably lower temperatures. Based on this idea, I started to fabricate the CO gas sensors with Pt-loaded CeO_2–ZrO_2–MO_x solid solution (M = Sn, Zn) to investigate their sensing performances (**Chapter 1**). Since the rapid response to CO is important for the practical sensor, I also tried to improve the response time of the sensor incorporating Pt-loaded CeO_2–ZrO_2–MO_x solid solution (M = Sn, Zn) by applying the low specific-heat material as the heat

transfer layer (**Chapter 2**). Moreover, from the viewpoint of reduction of the precious metal consumption, I employed Pt-free catalyst as a sensor material and established CO gas sensor without precious metal containing catalyst (**Chapter 3**).

The catalytic combustion-type gas sensor quantitatively detects CO gas by the electrical resistance change of Pt coil which is triggered by combustion of CO on the catalyst. A linear relationship is recognized between CO concentration and electrical resistance change of Pt coil as explained below.

When CO gas is combusted on oxidizing catalyst, the reaction heat (Q) raises temperature of Pt coil. If the temperature change of Pt (ΔT) is in a small range, the relationship between ΔT and Q is expressed by the following equation.

$$Q = (m_1 \cdot c_1 + m_2 \cdot c_2) \cdot \Delta T \tag{1-1}$$

(m_1 : mass of Pt, c_1 : heat capacity of Pt, m_2 : mass of catalyst, c_2 : heat capacity of catalyst)

The temperature change of Pt (ΔT) makes insulation resistivity change of Pt ($\Delta\rho$) with the relationship described by the following equation.

$$\Delta\rho = \rho(T_0) \cdot \alpha \cdot \Delta T \tag{1-2}$$

($\rho(T_o)$: initial insulation resistivity, α : temperature coefficient of Pt (3.9×10^{-3}/°C))

Then, the resistance change of Pt (ΔR) can be represented by the following equation.

$$\Delta R = L \cdot \Delta\rho / S \tag{1-3}$$

(L : length of Pt wire, S : sectional area of Pt wire)

On the other hand, the generated combustion heat (Q) is also represented by CO concentration (C) and gas volume (V) as the following equation.

$$Q = C \cdot V \cdot H \tag{1-4}$$

(H : combustion heat of CO per volume)

The four equations shown above give the following relationship.

$$\Delta R = L \cdot \rho(T_0) \cdot \alpha \cdot C \cdot V \cdot H / S \cdot (m_1 \cdot c_1 + m_2 \cdot c_2) \tag{1-5}$$

Because the values in the equation (1-5) are all constant except CO concentration (C), eq. (1-5) can be simplified to eq. (1-6).

$$\Delta R = k\,(\text{constant}) \times C \tag{1-6}$$

This equation means that the catalytic combustion-type sensor detects theoretically the CO gas concentration as the electrical resistance change of Pt coil. Therefore, measurement of ΔR as a function of CO concentration is essential to evaluate the sensing performance.

List of publications

1. Low-temperature operative carbon monoxide gas sensor with novel CO oxidizing catalyst

   A. Hosoya, S. Tamura, and N. Imanaka

   Chem. Lett., 2013, **42**, 441 – 443.

2. A Catalytic combustion-type CO gas sensor incorporating aluminum nitride as an intermediate heat transfer layer for accelerated response time

   A. Hosoya, S. Tamura, and N. Imanaka

   J. Sens. Sens. Syst., 2014, **3**, 141 – 144.

3. Catalytic combustion-type CO sensor applying Pt loaded CeO_2–ZrO_2–ZnO solid solution

   A. Hosoya, S. Tamura, and N. Imanaka

   J. Ceram. Soc. Jpn., 2014, **122**, 601 – 603.

4. A new catalytic combustion-type carbon monoxide gas sensor employing precious metal-free CO oxidizing catalyst

   A. Hosoya, S. Tamura, and N. Imanaka

   ISIJ Int., 2015, **55**, 1699 – 1701.

5. A catalytic combustion-type carbon monoxide gas sensor incorporating an apatite-type oxide

   A. Hosoya, S. Tamura, and N. Imanaka

   ISIJ Int., 2016, **56**, 1634 – 1637.

Chapter 1

Low temperature operative carbon monoxide gas sensors employing Pt-loaded CeO_2–ZrO_2–MO_x (M = Sn, Zn) solids

1.1 Introduction

In order to realize the low temperature operation of the catalytic combustion-type CO gas sensor, I focused on the Pt-loaded CeO_2–ZrO_2–MO_x solids (M = Sn, Zn) as the CO oxidation catalyst. Tin ion has both tetravalent (+4) and divalent (+2) states, and the $Ce_{1-x}Sn_xO_2$ solids have been reported to possess high oxygen storage and release properties compared with pure CeO_2 and SnO_2.[19-21] Therefore, the introduction of a small amount of SnO_2 into the CeO_2–ZrO_2 lattice will help to enhance the co-catalytic effect of the CeO_2–ZrO_2 solid caused by the intentional generation of oxide anion vacancy in the solid, suggesting that the sensors can work at lower temperatures. On the other hand, ZnO is accepted as n-type semiconductor same as the SnO_2, and electronic conduction is often observed for the ZnO doped oxides. Such electronic conduction would lead the valence change of cationic species, in this case, Ce in the CeO_2–ZrO_2 solid and subsequently generate the oxide anion vacancy in the solid. Therefore, the Pt-loaded CeO_2–ZrO_2–ZnO solid is also expected to show high catalytic activity toward CO.

In this chapter, fabrication of the sensors by incorporating the 10 wt% Pt/$Ce_{0.68}Zr_{0.17}Sn_{0.15}O_{2.0}$ or 10 wt% Pt/$Ce_{0.76}Zr_{0.19}Zn_{0.05}O_{1.95}$ solid as the catalyst investigation of the CO sensing performance at temperature as low as 70 °C are described.

1.2 Experimental Procedure

The $Ce_{0.68}Zr_{0.17}Sn_{0.15}O_{2.0}$ solid solution was prepared via the sol-gel method. SnC_2O_4 was dissolved in a mixture of aqueous solutions of 1.0 mol dm^{-3} $Ce(NO_3)_3$ and 0.1 mol dm^{-3} $ZrO(NO_3)_2 \cdot 2H_2O$ such that stoichiometric ratios between the reactants were achieved, following which aqueous solutions of 1.0 mol dm^{-3} citric acid and 30 w/v% acetic acid were added to the solution. Polyvinylpyrrolidone (PVP) was dissolved in the resulting mixture as a dispersant, after which the solution was stirring at 80 °C for 6 h. After then, the solvent was removed at 180 °C and the resulting powder was dried at 80 °C for 6 h, heated to 350 °C for 8 h to remove residual carbon and then calcined at 500 °C for 1 h in atmospheric air. The $Ce_{0.76}Zr_{0.19}Zn_{0.05}O_{1.95}$ solid solution was prepared via sol-gel method. After mixing a stoichiometric amount of aqueous solutions of 1.0 mol dm^{-3} $Ce(NO_3)_3$, 0.1 mol dm^{-3} $ZrO(NO_3)_2 \cdot 2H_2O$ and 1.0 mol dm^{-3} $Zn(NO_3)_2$, polyvinylpyrrolidone (PVP) was added into mixed solution. After the solution was stirring at 80 °C for 6 h, the solvent was removed at 180 °C and the resulting powder was dried at 80 °C for 6 h. The obtained powder was heated at 350 °C for 8 h to remove residual carbon without occurring any solid state reactions. After then, obtained powder was calcined at 500 °C for 1 h in atmospheric air.

10 wt% $Pt/Ce_{0.68}Zr_{0.17}Sn_{0.15}O_{2.0}$ and 10 wt% $Pt/Ce_{0.76}Zr_{0.19}Zn_{0.05}O_{1.95}$ were obtained by impregnating the $Ce_{0.68}Zr_{0.17}Sn_{0.15}O_{2.0}$ and $Ce_{0.76}Zr_{0.19}Zn_{0.05}O_{1.95}$ solid with a colloidal platinum solution stabilized with PVP. The catalyst was subsequently dried at 80 °C for 6 h and then calcined at 400 °C for 4 h in air.

Sample characterization was performed using X-ray fluorescence (Rigaku, ZSX100e), X-ray powder diffraction (XRD) (Rigaku, SmartLab). The CO oxidation activity was determined using a conventional fixed-bed flow reactor, by flowing 1 % CO in argon at a rate of 67 cm^3 min^{-1} over 0.2 g of catalyst, equivalent to a space velocity (S.V.) over the catalyst of 20,000 cm^3 h^{-1} g^{-1}. Prior to these activity measurements, the catalyst was heated at 200 °C for 2 h under an argon flow. The

oxidation activity was evaluated by the average amount of the approximately-constant CO conversion at each temperature maintained for over half an hour. The gas composition after the reaction was analyzed using a gas chromatograph with a thermal conductivity detector (TCD; Shimadzu, GC-8AIF).

The CO gas sensor was fabricated using a coil formed from 30 μm diameter Pt wire. A quantity of the 10 wt% Pt/$Ce_{0.68}Zr_{0.17}Sn_{0.15}O_{2.0}$ or 10 wt% Pt/$Ce_{0.76}Zr_{0.19}Zn_{0.05}O_{1.95}$ catalyst was dispersed in ethylene glycol respectively to form a slurry which was applied as a coating to the Pt coil. The coil was subsequently heated at approximately 150 °C for 30 s to drive off the ethylene glycol and sinter the catalyst. The CO gas detecting performance of the sensor was assessed using an electrometer (Advantest, R8240) to measure the DC voltage generated while passing a DC current of 90 mA through the sensor element to heat the cell to 70 °C (**Figure 1.1**). CO gas concentrations from 0 to 1000 ppm were produced by mixing 1000 ppm CO in air with dry air, and the mixed gas was direcrly introduced into the cell. Regardless of the CO gas concentration, the total gas flow rate passing over the sensor was kept constant at 40 mL min^{-1}. The sensor signal in response to CO gas

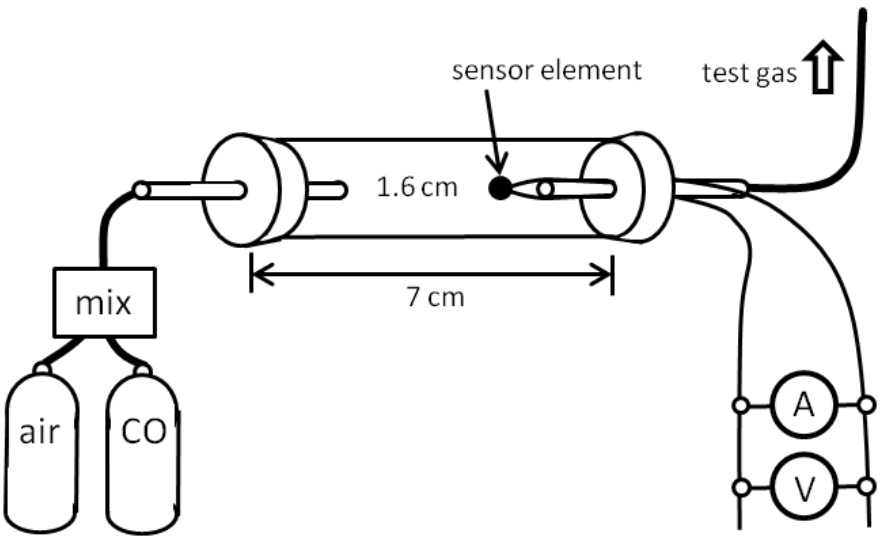

Figure 1.1 Schematic illustration of the set-up of the sensor element.

was defined as $(R_{gas}-R_{air})/R_{air}$, where R_{gas} and R_{air} are the electrical resistance of the sensor when in contact with gas containing CO and with pure air, respectively. The sensor response time (90% response time or 50% response time), which includes the gas substitutio time (approximately or more than 15 s) in the test chamber, was defined as the time required for the electrical resistance of the device to reach 90% or 50% of the equilibrium value eventually obtained at a given CO gas level.

1.3 Results and Discussion

1.3.1 CO gas sensor employed 10 wt% Pt/$Ce_{0.68}Zr_{0.17}Sn_{0.15}O_{2.0}$

The cationic ratio in the synthesized material was confirmed to be almost identical to that expected from the mixing ratio of reactants by X-ray fluorescence analysis as tabulated in **Table 1.1**. Furthermore, I confirmed the present catalyst had a comparatively high specific surface area of 77 $m^2\ g^{-1}$.

Table 1.1 The X-ray fluorescence analysis result and the BET surface area of the 10 wt% Pt/$Ce_{0.68}Zr_{0.17}Sn_{0.15}O_{2.0}$ solid

Estimated composition	Analyzed composition	BET surface area / $m^2\ g^{-1}$
10 wt% Pt/$Ce_{0.68}Zr_{0.17}Sn_{0.15}O_{2.0}$	10.2wt%Pt/$Ce_{0.71}Zr_{0.16}Sn_{0.13}O_{2.0}$	77

Figure 1.2 shows the XRD pattern of the 10 wt% Pt/$Ce_{0.68}Zr_{0.17}Sn_{0.15}O_{2.0}$ solid. The diffraction pattern exhibits only peaks assigned to the cubic fluorite-type oxide and metallic Pt without any crystalline impurities, and the diffraction peak angle of the cubic fluorite structure is slightly shifted to higher angles as compared to that of $Ce_{0.8}Zr_{0.2}O_{2.0}$, suggesting that the Ce^{4+} (ionic radius: 0.097

nm [22]) and Zr^{4+} (0.084 nm [22]) ions in the CeO_2–ZrO_2 solid is partially substituted with smaller Sn^{4+} ions (0.081 nm) [22] to form a solid solution. From these results, I concluded that the 10 wt% Pt loaded $Ce_{0.68}Zr_{0.17}Sn_{0.15}O_{2.0}$ solid solution was successfully obtained.

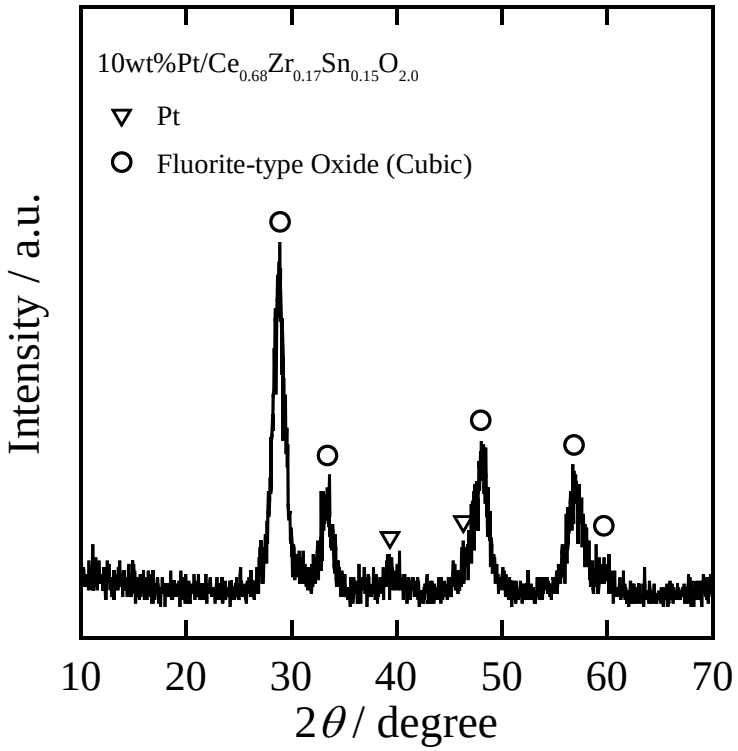

Figure 1.2 XRD pattern of synthesized 10 wt% $Pt/Ce_{0.68}Zr_{0.17}Sn_{0.15}O_{2.0}$ solid.

Figure 1.3 depicts the CO conversion properties of the 10 wt% Pt loaded $Ce_{0.68}Zr_{0.17}Sn_{0.15}O_{2.0}$ solid as a function of temperature. The 10 wt% Pt loaded $Ce_{0.68}Zr_{0.17}Sn_{0.15}O_{2.0}$ solid can oxidize CO at temperatures somewhat above 35 °C and that complete oxidation is achieved at 65 °C. Such high CO oxidation activity is considered to be realized by the co-catalytic effect of the $Ce_{0.67}Zr_{0.18}Sn_{0.25}O_{2.0}$ promoter. Lattice oxygen in the promoter may migrate easily to the surface through the lattice oxygen vacancies which is generated by the doping of a certain amount of Sn^{2+} ion [15]. As a result, oxygen migrated to the surface also work for the CO oxidation.

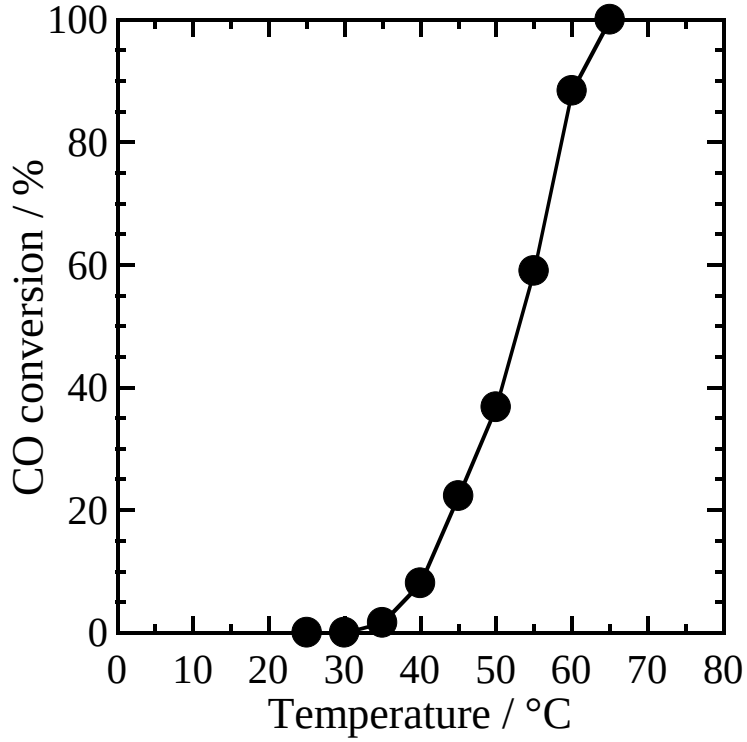

Figure 1.3 CO conversion performance of the 10 wt% Pt/$Ce_{0.68}Zr_{0.17}Sn_{0.15}O_{2.0}$ solid.

Although I tried to operate the sensor with the 10 wt% Pt/$Ce_{0.68}Zr_{0.17}Sn_{0.15}O_{2.0}$ solid at 65 °C that is the threshold temperature where this catalyst can completely oxidize CO (**Figure 1.2**), the sensor signal contained a high level of electrical noise. The reason why the sensor did not show the stable sensor signal at 65 °C is considered to be due to the very small amount (less than 0.6 mg) of catalyst loaded over the Pt coil, which may be insufficient amount to produce the reliable level of combustion heat. When the sensor operation temperature was raised to 70 °C, however, stable sensing performance was successfully obtained, presumably due to the acceleration of oxidation performance of the catalyst by the temperature increase. **Figure 1.4** presents a representative sensor response curve obtained when the CO gas concentration was varied from 0 to 1000 ppm and back again in a step-by-step manner at 70 °C. It is evident that the sensor signal ($(R_{gas}-R_{air})/R_{air}$) changed

smoothly and reproducibly with varying CO gas concentration, with a 90% response time of less than 10 min. However, based on the size of the test chamber and the gas flow rate, and taking into account the lag time required to fully equilibrate the chamber to changes in CO gas concentration, the actual response time is estimated at approximately 3 min (including gas substitution time: more than 15 s).

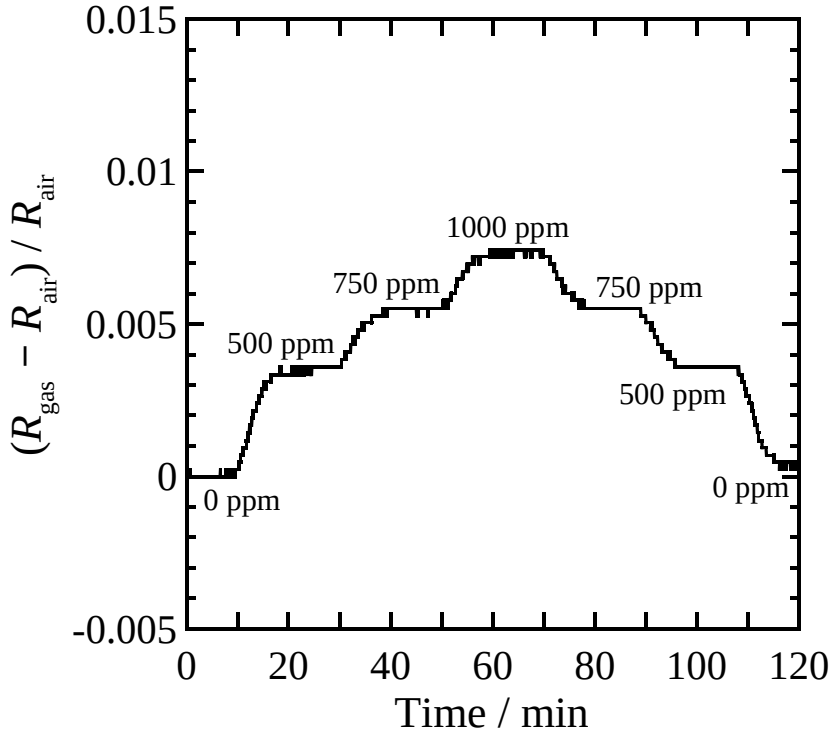

Figure 1.4 Representative sensor response curve obtained by varying CO concentration from 0 to 1000 ppm and back at 70 °C for the sensor with 10 wt% $Pt/Ce_{0.68}Zr_{0.17}Sn_{0.15}O_{2.0}$ solid.

Figure 1.5 shows the equilibrium sensor signals obtained at 70 °C in response to various CO gas concentrations. The sensor signal varies in a strictly linear fashion with changing CO gas concentration, and the same signal was obtained for identical CO gas levels both on increasing and decreasing the concentration, indicating that the device response is both stable and reproducible. From these results, it can be concluded that the present sensor incorporating the 10 wt% $Pt/Ce_{0.68}Zr_{0.17}Sn_{0.15}O_{2.0}$ solid as a CO oxidation catalyst can detect CO gas even at 70 °C which is considerably lower than the temperature required for the operation of sensors using a conventional catalyst such as Pt/Al_2O_3 or Pd/Al_2O_3 (approximately 400°C).

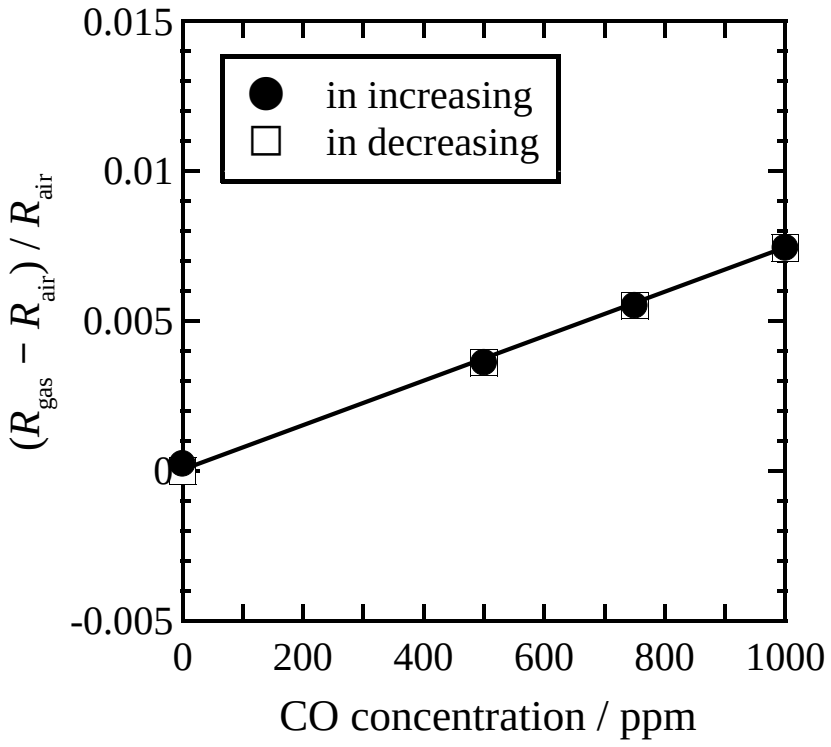

Figure 1.5 Relationship between CO gas concentration and sensor signal obtained at each level of CO gas concentration at 70 °C for the sensor with 10 wt% $Pt/Ce_{0.68}Zr_{0.17}Sn_{0.15}O_{2.0}$ solid.

1.3.2 CO gas sensor employed 10 wt% Pt/$Ce_{0.76}Zr_{0.19}Zn_{0.05}O_{1.95}$

Figure 1.6 shows the XRD pattern of the 10 wt% Pt/$Ce_{0.76}Zr_{0.19}Zn_{0.05}O_{1.95}$ solid. Only peaks assigned to the cubic fluorite-type oxide and metallic Pt were observed with no crystalline impurities. Similar to the case for the 10 wt% Pt/$Ce_{0.68}Zr_{0.17}Sn_{0.15}O_{2.0}$ solid, the diffraction peaks assigned to the cubic fluorite-type structure were shifted slightly to higher angles as compared to the pattern for the mother solid of $Ce_{0.8}Zr_{0.2}O_{2.0}$, suggesting that the Ce^{4+} (ionic radius: 0.097 nm [22]) and Zr^{4+} (0.084 nm [22]) ions in CeO_2–ZrO_2 (estimated avarage ionic radius of $0.8Ce^{4+}$–$0.2Zr^{4+}$: 0.0944 nm) have been partially substituted with smaller Zn^{2+} ions (0.09 nm [22]) to form a solid solution. Furthermore, I have confirmed the composition of the synthesized solid by X-ray fluorescence analysis to be almost identical to the expected one from the mixing ratio of the reactants as listed in **Table 1.2**. Furthermore, the BET surface area of 10 wt%

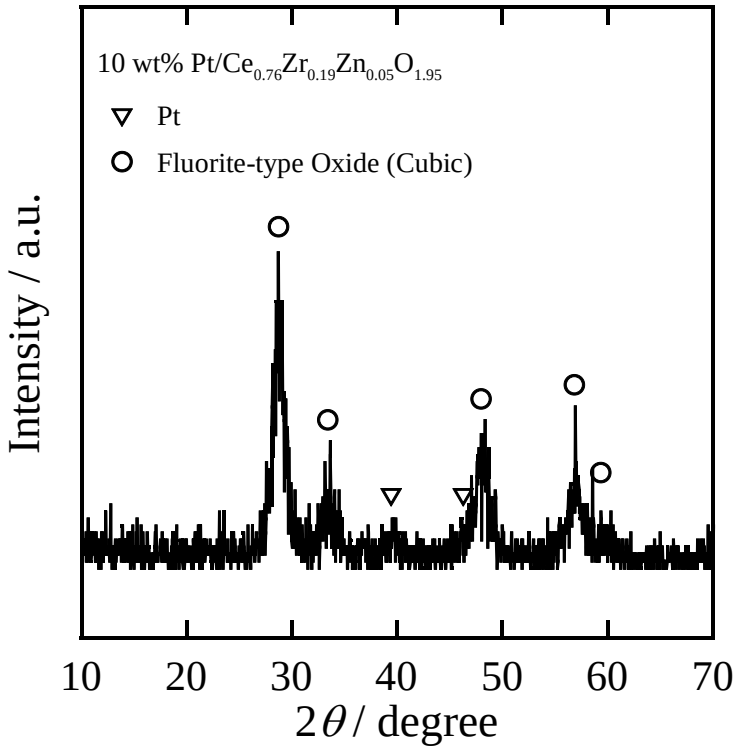

Figure 1.6 XRD pattern of synthesized 10 wt% Pt/$Ce_{0.76}Zr_{0.19}Zn_{0.05}O_{1.95}$ solid.

$Pt/Ce_{0.68}Zr_{0.17}Sn_{0.15}O_{2.0}$ solid was almost the same as that of 10 wt% $Pt/Ce_{0.68}Zr_{0.17}Sn_{0.15}O_{2.0}$ solid. From these results, it was confirmed that the 10 wt% $Pt/Ce_{0.76}Zr_{0.19}Zn_{0.05}O_{1.95}$ solid solution was successfully obtained.

Table 1.2 The X-ray fluorescence analysis result and the BET surface area of the 10 wt% $Pt/Ce_{0.76}Zr_{0.19}Zn_{0.05}O_{1.95}$ solid

Estimated composition	Analyzed composition	BET surface area / $m^2\ g^{-1}$
10 wt% $Pt/Ce_{0.76}Zr_{0.19}Zn_{0.05}O_{1.95}$	10.3wt%$Pt/Ce_{0.80}Zr_{0.17}Zn_{0.04}O_{1.96}$	72

Figure 1.7 depicts the CO conversion properties of the 10 wt% $Pt/Ce_{0.76}Zr_{0.19}Zn_{0.05}O_{1.95}$ catalyst. The 10 wt% $Pt/Ce_{0.76}Zr_{0.19}Zn_{0.05}O_{1.95}$ catalyst showed CO oxidizing activity quite low temperature

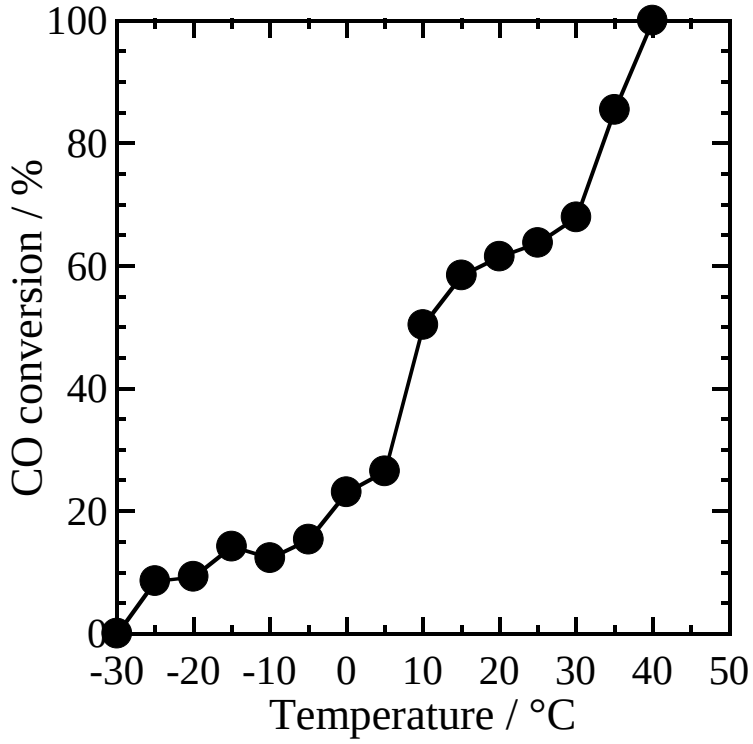

Figure 1.7 CO conversion for catalyst as a function of temperature.

of even at −25 °C and complete oxidation was realized at such a temperature of 40 °C. Since the sensor with 10 wt% Pt/$Ce_{0.68}Zr_{0.17}Sn_{0.15}O_{2.0}$ solid (discussed in **1.3.1**) which exhibited a complete CO oxidation at 65 °C realized a sensor operation at 70 °C, the sensor with the 10 wt% Pt/$Ce_{0.76}Zr_{0.19}Zn_{0.05}O_{1.95}$ catalyst can be also expected to operate at low temperatures. Such higher CO oxidation activity of 10 wt% Pt/$Ce_{0.76}Zr_{0.19}Zn_{0.05}O_{1.95}$ catalyst compared with the 10 wt% Pt/$Ce_{0.68}Zr_{0.17}Sn_{0.15}O_{2.0}$ catalyst is thought to be caused by the high amount of oxide ion vacancy generated in the solid which is produced by the lower valence state of Zn (+2) compared to that of Sn (+4). High amount of oxide ion vacancy would accelerate the oxidation reaction on the catalyst surface by using oxygen migrated from inside the lattice to the surface.

Figure 1.8 presents a representative sensor response curve obtained when the CO gas concentration was varied from 0 to 1000 ppm and vice versa in a step-by-step manner at the temperature of 70 °C. The sensor signal ($(R_{gas}-R_{air})/R_{air}$) changed smoothly and reproducibly with

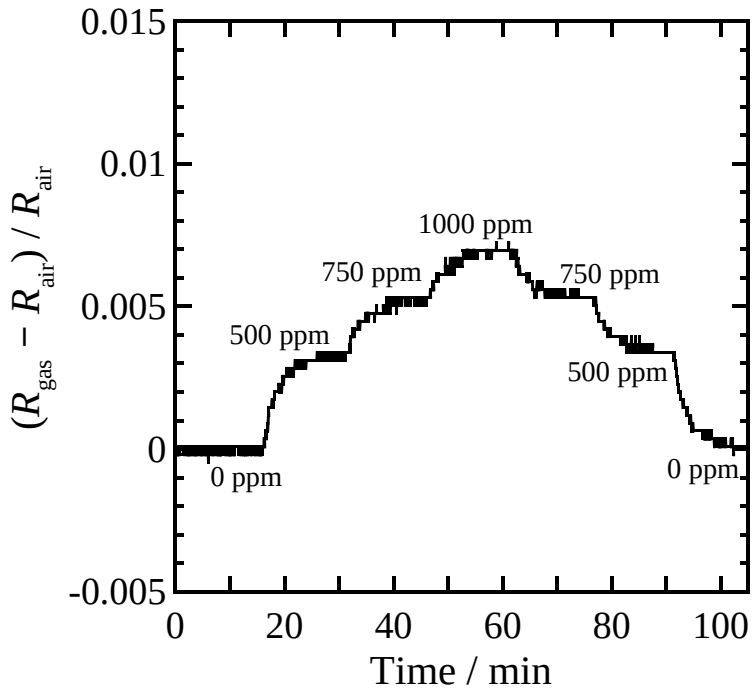

Figure 1.8 Representative sensor response curve obtained by varying CO concentration from 0 to 1000 ppm and back at 70 °C.

varying CO gas concentration. The 90% response time estimated from the response curve was approximately 3–4 min including the gas substitution time (more than 15 s), which was similar to the sensor with the 10 wt% Pt/$Ce_{0.68}Zr_{0.17}Sn_{0.15}O_{2.0}$ solid (discussed in **1.3.1**).

Figure 1.9 shows the CO gas concentration dependence of the sensor signal obtained at 70 °C. The sensor signal changed linearly with varying CO gas concentration, and the same value was obtained for identical CO gas levels both in increasing and in decreasing steps of the concentration, indicating that the stable and reproducible sensor response is obtained for the sensor with 10 wt% Pt/$Ce_{0.76}Zr_{0.19}Zn_{0.05}O_{1.95}$ catalyst at 70 °C. Although the operation temperature of the sensor incorporating the 10 wt% Pt/$Ce_{0.76}Zr_{0.19}Zn_{0.05}O_{1.95}$ catalyst, whose CO complete oxidation temperature is 40 °C which is lower than that of 10 wt% Pt/$Ce_{0.68}Zr_{0.17}Sn_{0.15}O_{2.0}$ solid (65 °C), can be expected to lower furthermore, the stable sensor signal without electrical noise coud not be

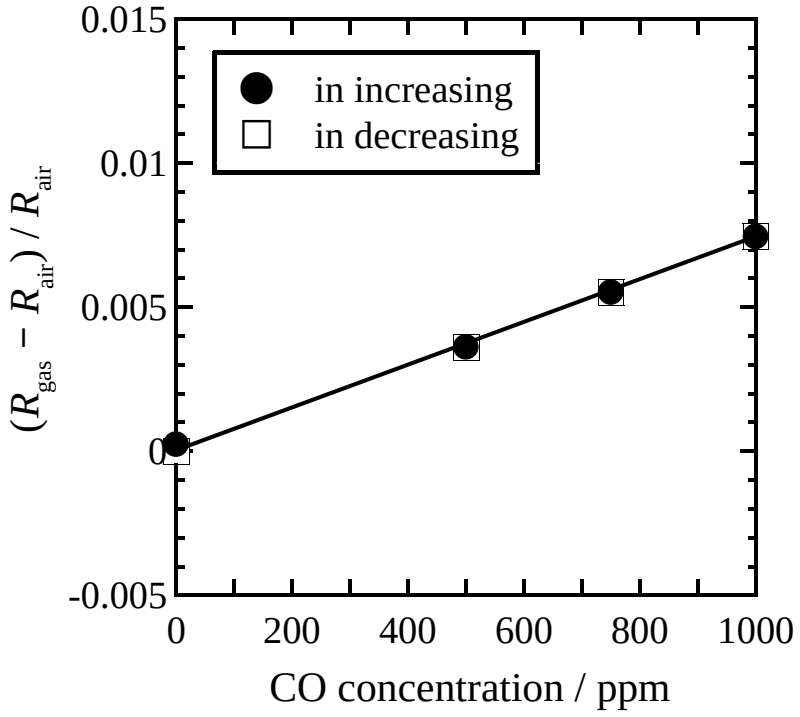

Figure 1.9 Relationship between CO gas concentration and sensor output obtained at each level of CO gas concentration.

obtained below 70 °C, similar to the case for the sensor with the 10 wt% Pt/$Ce_{0.68}Zr_{0.17}Sn_{0.15}O_{2.0}$ solid, due to the small amount of catalyst loaded onto the Pt coil.

1.4 Conclusion

I have fabricated the catalytic combustion type CO gas sensor, which can operate at lower temperatures, employing the 10 wt% Pt/$Ce_{0.68}Zr_{0.17}Sn_{0.15}O_{2.0}$ or 10 wt% Pt/$Ce_{0.76}Zr_{0.19}Zn_{0.05}O_{1.95}$ catalysts. Since the Pt-loaded CeO_2–ZrO_2–MO_x solid (M = Sn, Zn) catalysts have high CO oxidizing activity even at moderate temperatures below 65 °C, the sensors with these catalysts exhibited continuous and reproducible response toward CO at as low as 70 °C, which is about 300 °C lower than that for the conventional catalytic combustion-type CO gas sensors with Pt or Pd loaded Al_2O_3. Moreover, since the sensor signal of the present sensors was proportionally changed to the CO gas concentration variation, it was found that the sensors with the Pt-loaded CeO_2–ZrO_2–MO_x solid (M = Sn, Zn) catalysts can detect CO quantitatively.

Chapter 2

Improvement of response time of the catalytic combustion-type CO gas sensor with 10 wt% Pt/$Ce_{0.68}Zr_{0.17}Sn_{0.15}O_{2.0}$

2.1 Introduction

As described in **Chapter 1**, I have succeeded in developing the catalytic combustion-type CO gas sensor which can operate at as low as 70 °C by incorporating the 10 wt% Pt/$Ce_{0.68}Zr_{0.17}Sn_{0.15}O_{2.0}$ or 10 wt% Pt/$Ce_{0.76}Zr_{0.19}Zn_{0.05}O_{1.95}$ solids as the CO oxidizing catalyst. Although the low temperature sensor operation has been achieved, its 90% response time was as long as 3 min which has to be shorten to prevent the serious accidents caused by the CO exposure. Since the slow response of the sensor with Pt-loaded CeO_2–ZrO_2–MO_x catalysts is considered to be due to insufficient heat transfer from the catalyst to the Pt coil, it is essential to improve the heat transfer property of the sensor element.

In this chapter, an attempt to improve the sensing response time is described. The key technique is employment of the thermoelectric material of aluminum nitride (AlN) as an intermediate heat transfer layer. Aluminum nitride is a representative material which possess low specific-heat coefficient. To investigate the effect of the AlN layer to the sensing performance, especially to the response time, I selected the 10 wt% Pt/$Ce_{0.68}Zr_{0.17}Sn_{0.15}O_{2.0}$ catalyst because the sensor with the 10 wt% Pt/$Ce_{0.68}Zr_{0.17}Sn_{0.15}O_{2.0}$ catalyst showed slightly rapid and stable response compared to that with 10 wt% Pt/$Ce_{0.76}Zr_{0.19}Zn_{0.05}O_{1.95}$ catalyst.

2.2 Experimental Procedure

Figure 2.1 illustrates the CO gas sensor element fabricated with the AlN lyaer. AlN (D_{50}: 13.4 μm, BET surface area: 0.9 m^2g^{-1}, Toyo Aluminum K. K.) was dispersed first in ethylene glycol to form a slurry which was painted over the Pt coil, and then ethlene glychol was drived off by applying a dc voltage of 3 V to heat the Pt coil. Subsequently, the 10 wt% Pt/$Ce_{0.68}Zr_{0.17}Sn_{0.15}O_{2.0}$ catalyst was dispersed in ethylene glycol and was applied over top of the AlN layer on the Pt coil. The coil was then heated in the same way to drive off the ethylene glycol and sinter the catalyst. To allow an assessment of the efficiency of the AlN as an intermediate heat transfer layer, the total weight of AlN and catalyst applied was kept constant (0.6 mg) to compare the sensing performance with the sensor without AlN (**Chapter 1**). The CO sensing performance of the sensor was investigated using an electrometer (Advantest, R8240) to measure the DC voltage generated while passing a DC current of 90 mA through the sensor element to heat the cell up to 70 °C. CO gas concentrations from 0 to 500 ppm were produced by diluting 1000 ppm CO in air with dry air. Regardless of the CO gas concentration, the total gas flow rate passing over the sensor was kept constant at 40 mL min^{-1}. The sensor signal in response to exposure to CO gas was defined as $(R_{gas}-R_{air})/R_{air}$, where R_{gas} and R_{air} are the electrical resistances of the sensor when in contact with

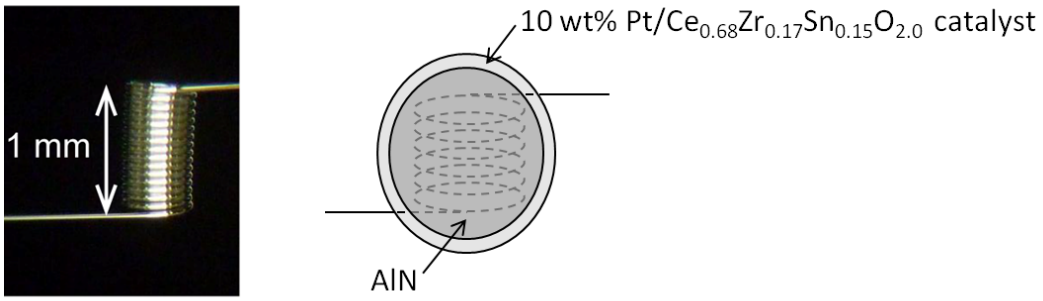

Figure 2.1 Schimatic illustration of the established sensor element.

gas containing CO and with pure air, respectively. The sensor response time was defined as the time required for the electrical resistance of the device to reach 90% or 50% of the equilibrium value eventually obtained at a given CO gas level.

2.3 Results and Discussion

The relationship between the amount of AlN and its effect on the CO gas detecting properties of the established sensors was investigated. **Table 2.1** tabulates the 90% response time and sensor signal for 500 ppm CO. As increasing the amount of AlN, both the response time and the sensor signal improved. Although I tried to fabricate the sensor element with much amount of AlN, I could not establish the sensor element covered by a reliable amount of catalyst because the weight of catalyst was less than 0.1 mg which is lowest weighing limit of electric balance used.

Table 2.1 90 % response time and sensor signal for 500 ppm CO of each sensor with different amount of AlN

10 wt% $Pt/Ce_{0.68}Zr_{0.17}Sn_{0.15}O_{2.0}$ catalyst : AlN (in weight ratio)	90% response time /s	sensor signal for 500 ppm CO
1 : 5	< 90	0.0054
1 : 1	100 – 120	0.0050
5 : 1	100 – 140	0.0044
without AlN (**Chapter 1**)	approx. 180	0.0036

Figure 2.2 exhibits a representative response curve for the present sensor with the AlN intermediate heat transfer layer (weight ratio of catalyst and AlN is 1:5.) at 70 °C. The sensor with

AlN showed more stable output and sharp response to CO gas concentration change, and the 90% response time was drastically shortened to within 90 s compared to the sensor without AlN (approx. 180 s). Furthermore, the 50% response time is 20 – 30 s (with experimental error of 10 s) while the sensor without AlN required over 130 s for a 50% response. In addition, clear sensor signal was obtained even in quite low CO concentration (125 ppm), indicating that the sensitivity of the sensor was improved by applying the heat conductive material of AlN having a low heat capacity.

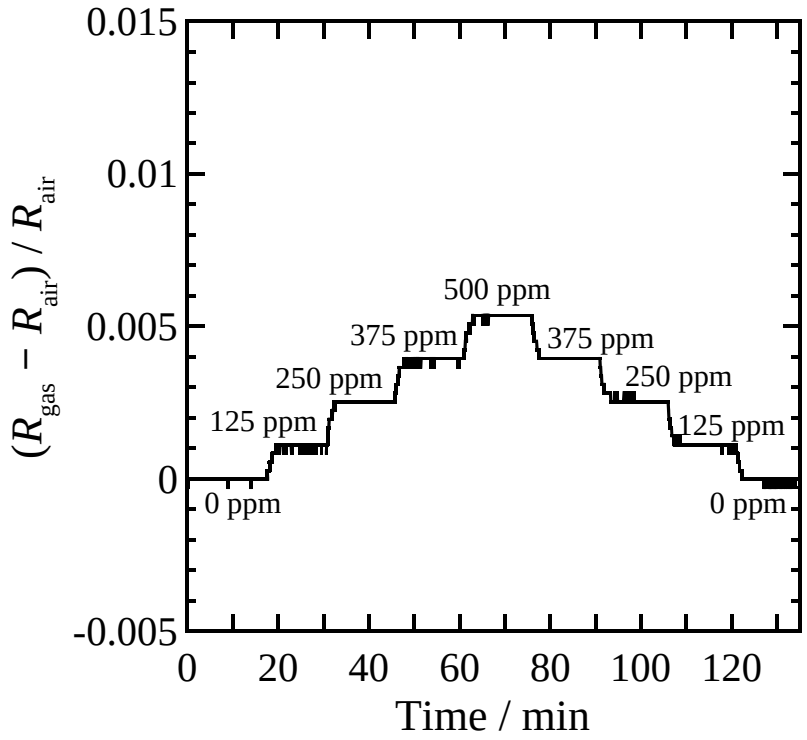

Figure 2.2 Representative sensor response curve obtained by varying CO concentration from 0 to 500 ppm and back at 70 °C.

Figure 2.3 depicts the sensor signals obtained at 70 °C in response to various CO gas concentrations. A sensor without AlN which was described in **Chapter 1**, the sensor with AlN also produced a signal which varies in a linear relationship with changing CO gas concentrations. Moreover, the sensitivity of the sensor with AlN is higher than that of the sensor without AlN; the sensor signal of the sensor with AlN to 500 ppm CO is approx. 1.5 times higher than that of the sensor without AlN.

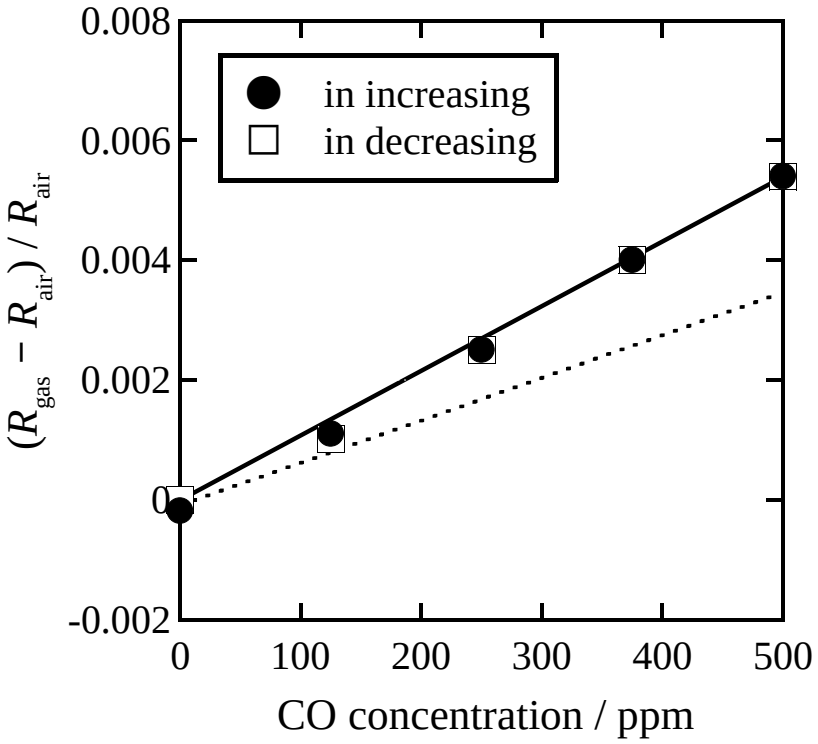

Figure 2.3 Relationship between CO gas concentration and sensor signal obtained at each level of CO gas concentration. The dashed line is corresponding data of the previously discussed sensor (in **Chapter 1**).

Since the sensor components, except for the presence of the AlN interlayer, are the same to the previously discussed sensor (**Chapter 1**), acceleration of the response time should be due to the

improvement of the heat transfer from the CO oxidizing catalyst to the Pt coil. In the case of the sensor without the AlN interlayer, a quantity of heat generated by CO oxidation on the catalyst will be released into atmospheric air before it conducts to the Pt coil. As a result, a prolonged time is necessary to reach a thermal equilibrium state in the Pt coil. In contrast, by introducing the AlN interlayer, a greater quantity of heat is effectively and rapidly conducted to the Pt coil through the AlN layer due to its excellent thermal conductivity. This results in both a steady sensor signal and a rapid response. The sensitivity was also improved by applying AlN as the heat transfer layer, because the heat capacity of AlN is less than that of the 10 wt% Pt/$Ce_{0.68}Zr_{0.17}Sn_{0.15}O_{2.0}$ catalyst. The temperature of a material with a lower heat capacity will increase to a greater extent in response to the same amount of heat energy and therefore the temperature of the Pt coil is further increased as the heat generated in the catalyst is conducted through the AlN layer. Because the sensor signal is dependent on the electrical resistance of the Pt coil, which in turn is directly related to the temperature of the Pt, the sensitivity of the sensor with AlN was improved due to the lower heat capacity of the AlN compared to that of the catalyst. The results in this chapter indicate that the high thermal conductivity of AlN can improve CO sensing performance of the catalytic combustion-type sensor.

2.4 Conclusion

In order to improve the sensing response of the catalytic combustion-type CO gas sensor with Pt-loaded $Ce_{0.68}Zr_{0.17}Sn_{0.15}O_{2.0}$ catalyst, heat conductive material of aluminum nitride was inserted as the heat transfer layer between Pt coil and catalyst. The sensor inserted AlN layer exhibited rapid response and larger sensor signal as the amount of AlN increased. The sensor with 10 wt% $Pt/Ce_{0.68}Zr_{0.17}Sn_{0.15}O_{2.0}$ catalyst and AlN in the weight ratio of 1:5 exhibited the best CO detecting property of approximately 1/6 shorter 50% response time and approximately 1.5 times larger sensor signal compared to the sensor employed 10 wt% $Pt/Ce_{0.68}Zr_{0.17}Sn_{0.15}O_{2.0}$ catalyst without AlN layer which was discribed in **Chapter 1**.

Chapter 3

Catalytic combustion-type CO gas sensor with Pt-free catalyst

3.1 Introduction

I have succeeded in developing the low temperature (70 °C) operative catalytic combustion-type CO gas sensor by incorporating the 10 wt% Pt / $Ce_{0.68}Zr_{0.17}Sn_{0.15}O_{2.0}$ catalyst (**Chapter 1**) and have also improved its sensing response by introducing the heat transfer layer (**Chapter 2**). As a result of strategic selection of sensor components, I have realized the commercially applicable CO gas sensor possessing rapid response even at considerably low temperature. However, the catalyst employed contains precious metal of Pt whose consumed amount should be saved, and therefore, it is demanded to use the Pt-free catalyst in the light of practical use, especially in cost.

To fulfill such a demand, I focused on $LaCoO_3$ which has been reported to show catalytic activity toward CO oxidation whose activity was improved by loading on the supporter with high specific surface area.[23] On the other hand, I demonstrated the superiority of use the $Ce_{0.67}Zr_{0.18}Sn_{0.15}O_{2.0}$ solid in which the oxide anion conduction helps to oxidize the CO gas on the catalyst. Therefore, it is considered that the Pt-free CO oxidizing catalyst possessing reliable activity even at low temperatures can be realized by loading $LaCoO_3$ onto the $Ce_{0.67}Zr_{0.18}Sn_{0.15}O_{2.0}$ solid.

In this chapter, development of a catalytic combustion-type CO gas sensor using the $LaCoO_3$-loaded $Ce_{0.67}Zr_{0.18}Sn_{0.15}O_{2.0}$ catalyst and investigation of its sensing performance are describe.

3.2 Experimental Procedure

The $Ce_{0.68}Zr_{0.17}Sn_{0.15}O_{2.0}$ solid solution was synthesized by the sol-gel method, as described in **Chapter 1**. Then $LaCoO_3$ was loaded onto the $Ce_{0.68}Zr_{0.17}Sn_{0.15}O_{2.0}$ promoter to yield 15.9 wt% $La_{0.87}Co_{1.13}O_3$-loaded $Ce_{0.67}Zr_{0.18}Sn_{0.15}O_{2.0}$ catalyst by the following procedure: 0.36 g of $Ce_{0.68}Zr_{0.17}Sn_{0.15}O_{2.0}$ solid was added to the mixed solution of 3.0 mL of 0.1 mol L^{-1} $La(NO_3)_3$ and 3.0 mL of 0.1 mol L^{-1} $Co(NO_3)_2$. Then 1.26 mL of 1.0 mol L^{-1} cytric acid solution and ca. 10 mL of deionized water were added and the mixed solution was stirred for 5 h at room temperature. After then, the solvent was removed off at 80 °C by using hot stirrer and the obtained powder was heated at 140 °C for 1 h. The obtained powder was calcined at 700 °C for 6 h in air.

The sample synthesized was identified by X-ray fluorescence (Rigaku, ZSX100e) and X-ray powder diffraction (XRD) (Rigaku, SmartLab) analyses with the Cu-Kα line. CO oxidation activity of the 15.9 wt% $La_{0.87}Co_{1.13}O_3/Ce_{0.67}Zr_{0.18}Sn_{0.15}O_{2.0}$ catalyst was investigated by a conventional fixed-bed flow reactor by flowing 1000 ppm CO diluted with air at the space velocity of 20000 L kg^{-1} h^{-1}.

The sensor element was fabricated with AlN heat transfer layer in the same way as described in **Chapter 2**. The CO sensing performance of the sensor was investigated at 130 °C by using an electrometer (Advantest, R8240) in the atmosphere whose CO gas concentration was varied from 0 to 500 ppm that obtained by diluting 1000 ppm CO (air balance) gas with synthetic air. Regardless of the CO gas concentration, the total gas flow rate passing over the sensor was kept constant at 40 mL min^{-1}. The sensor signal in response to exposure to CO gas was defined as $(R_{gas}-R_{air})/R_{air}$, where R_{gas} and R_{air} are the electrical resistances of the sensor in the test gas containing CO and in pure air, respectively. The sensor response time was defined as the time required for the electrical resistance of the device to reach 50% or 90% of the steady value eventually obtained at a given CO gas level.

3.3 Results and Discussion

The cationic ratio (La : Co : Ce : Zr : Sn) in the prepared solid was confirmed to be almost identical to the mixing one of the reactants by X-ray fluorescence analysis (**Table 3.1**). Althought the BET surface area of the prepared catalyst is smaller than those of the Pt-loaded catalysts (**Tables 1.1 and 1.2**), due to the large particle size of LaCoO3 oxide compared with the Pt particle obtained from colloidal platinum solution stabilized with PVP, large surface area was still obtained. In the XRD pattern of the 15.9 wt% $La_{0.87}Co_{1.13}O_3$-loaded $Ce_{0.67}Zr_{0.18}Sn_{0.15}O_{2.0}$ (**Figure 3.1**), only peaks assigned to the cubic fluorite-type oxide and perobskite-type oxide without any crystalline impurities were clearly observed. Furthermore, the diffraction peak angles assigned to the cubic fluorite-type oxide were shifted slightly to higher angles as compared to those of $Ce_{0.8}Zr_{0.2}O_{2.0}$. These results clealy suggest that the celium (ionic radius of Ce^{3+}: 0.114 nm, Ce^{4+} : 0.097 nm [22]) ion sites in the $Ce_{0.8}Zr_{0.2}O_{2.0}$ were partially substituted with smaller tin ions (ionic radius of Sn^{2+}: 0.093 nm, Sn^{4+} : 0.071 nm [24]) to form a solid solution, and the 15.9 wt% $La_{0.87}Co_{1.13}O_3$-loaded $Ce_{0.67}Zr_{0.18}Sn_{0.15}O_{2.0}$ solid was successfully obtained.

Table 3.1 The X-ray fluorescence analysis result and the BET surface area of the 15.9 wt% $La_{0.87}Co_{1.13}O_3/Ce_{0.67}Zr_{0.18}Sn_{0.15}O_{2.0}$ solid

Estimated composition	Analyzed composition	BET surface area / $m^2\ g^{-1}$
15.9 wt% $La_{0.87}Co_{1.13}O_3$ / $Ce_{0.67}Zr_{0.18}Sn_{0.15}O_{2.0}$	15.9wt%$La_{0.87}Co_{1.13}O_3$/ $Ce_{0.67}Zr_{0.18}Sn_{0.15}O_{2.0}$	35.7

Figure 3.2 shows the CO oxidation activity of the 15.9 wt% $La_{0.87}Co_{1.13}O_3$-loaded $Ce_{0.67}Zr_{0.18}Sn_{0.15}O_{2.0}$ catalyst as a function of temperature. The present catalyst starts to oxidize CO

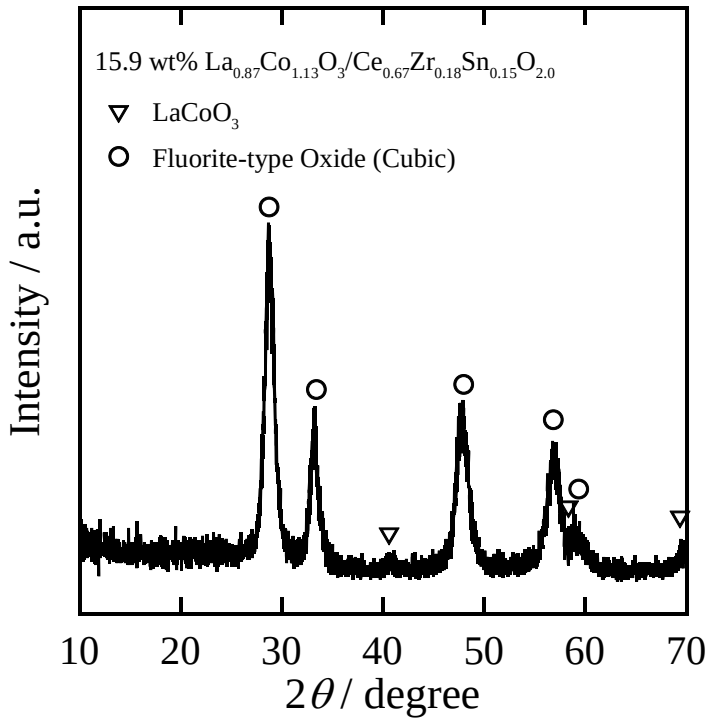

Figure 3.1 XRD pattern of synthesized 15.9 wt% $La_{0.87}Co_{1.13}O_3$-loaded $Ce_{0.67}Zr_{0.18}Sn_{0.15}O_{2.0}$.

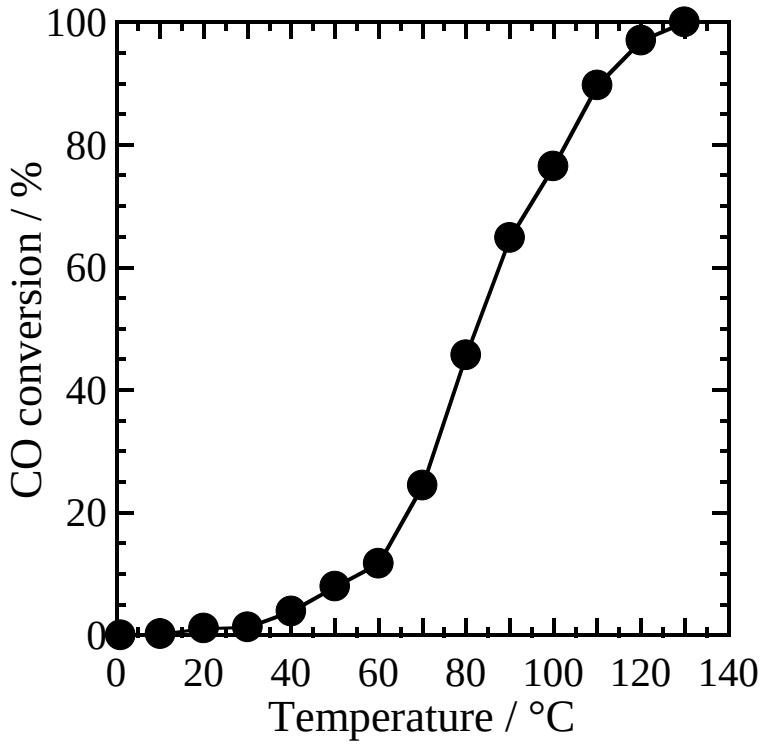

Figure 3.2 CO conversion for catalyst as a function of temperature.

at 30 °C and complete oxidation is realized at 130 °C. From this result, it was greatly expected that the sensor can detect CO gas concentration quantitatively around 130 °C even in the absence of precious metal of Pt.

Figure 3.3 displays a representative response curve for the present sensor incorporating the 15.9 wt% $La_{0.87}Co_{1.13}O_3/Ce_{0.67}Zr_{0.18}Sn_{0.15}O_{2.0}$ catalyst with AlN intermediate heat transfer layer when the CO gas concentration was varied from 0 to 500 ppm and vice versa in a step-by-step manner at 132 °C. The sensor signal ($(R_{gas}-R_{air})/R_{air}$) changed smoothly and reproducibly with varying the CO gas concentration, similar to the case for previously reported sensor with 10 wt% $Pt/Ce_{0.67}Zr_{0.18}Sn_{0.15}O_{2.0}$ catalyst. Furthermore, the 50% and the 90% response time were 20–40 s and 50–100 s, respectively, which are the comparable to the time (20–30 s and 90 s) obtained for the previously discussed sensor employing 10 wt% $Pt/Ce_{0.68}Zr_{0.17}Sn_{0.15}O_{2.0}$ and AlN intermediate layer [7] (**Chapter 2**).

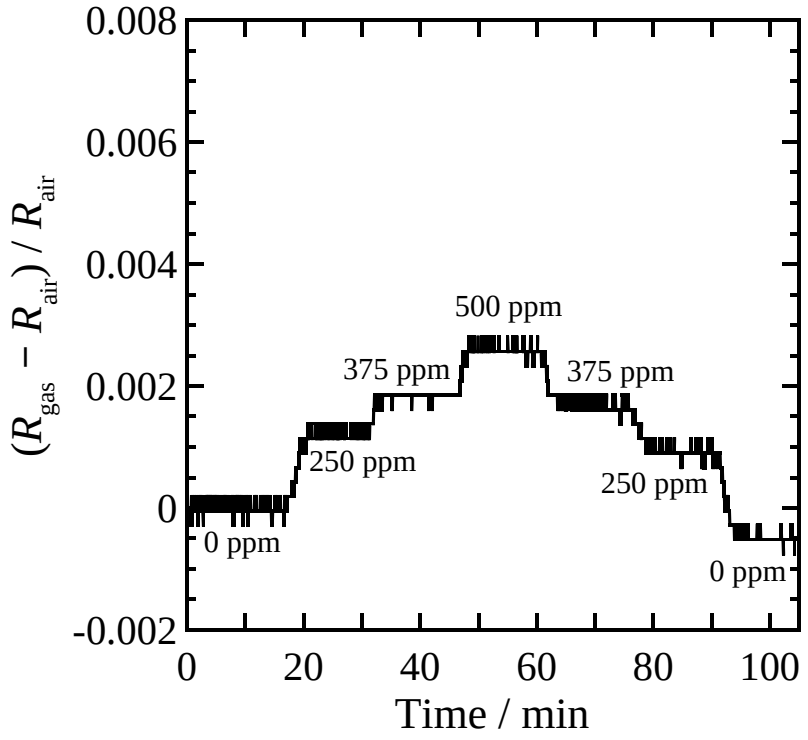

Figure 3.3 Representative sensor response curve obtained by varying CO concentration from 0 to 500 ppm and back at 130 °C.

Figure 3.4 depicts the steady-state sensor signals at various CO gas concentrations at 132 °C. Similar to the previous sensor reported in **Chapter 2**, the present sensor produces a signal which varies in a linear fashion with changing the CO gas concentration, suggesting that the present sensor can also detect CO concentration quantitatively. Although the operation temperature of the present sensor is higher than that of the previous sensor with Pt loaded catalyst (**Chapters 1 and 2**), it is quite lower than those (ca. 400 °C) of conventional sensors with precious metal-loading Pt/Al_2O_3 or Pd/Al_2O_3 catalyst. Moreover, the present sensor has a merit in cost because the sensor employed precious-metal free catalyst of 15.9 wt% $La_{0.87}Co_{1.13}O_3/Ce_{0.67}Zr_{0.18}Sn_{0.15}O_{2.0}$ having similar quick response to the sensor discussed in **Chapter 2**. From these advantages, the present sensor is considerd to be another candidate for the practical CO detecting tool.

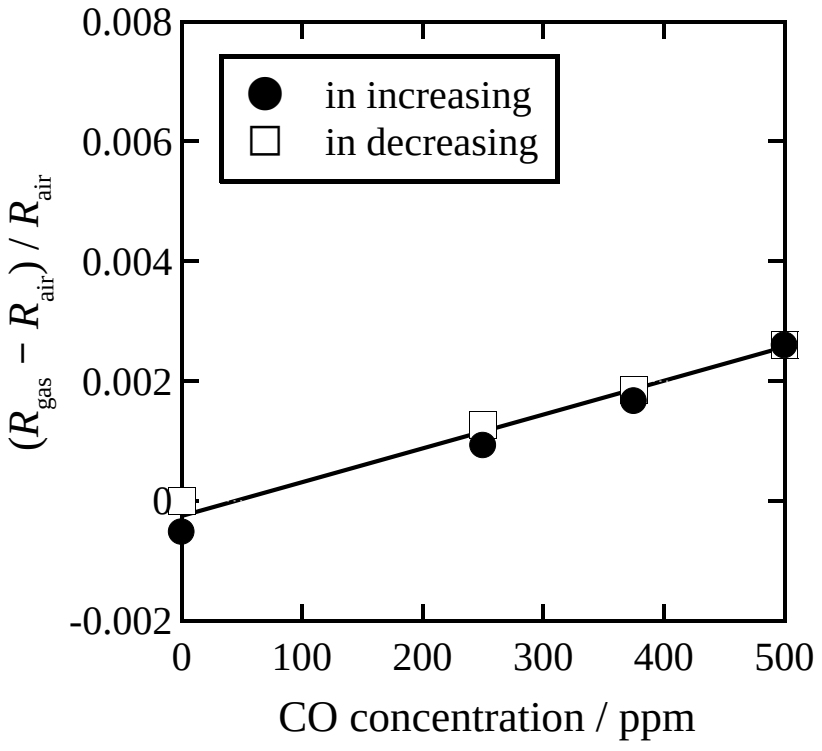

Figure 3.4 Relationship between CO gas concentration and sensor output obtained at each level of CO gas concentration.

3.4 Conclusion

In order to meet a demand of recent request to reduce the consumption of precious metal, I developed the precious metal-free catalyst of the $La_{0.87}Co_{1.13}O_3$-loaded $Ce_{0.67}Zr_{0.18}Sn_{0.15}O_{2.0}$ solid and applied it to a sensor component. Since the synthesized 15.9 wt% $La_{0.87}Co_{1.13}O_3$/ $Ce_{0.67}Zr_{0.18}Sn_{0.15}O_{2.0}$ catalyst possessed high catalytic activity whose complete CO oxidation temperature is 130 °C, the sensor incorporating 15.9 wt% $La_{0.87}Co_{1.13}O_3$/$Ce_{0.67}Zr_{0.18}Sn_{0.15}O_{2.0}$ catalyst with AlN exhibited continuous and reproducible response toward CO at temperature of 130 °C, which is even lower than that for the conventional catalytic combustion-type CO sensor with Pt or Pd loaded Al_2O_3.

Summary

In this thesis, I focused on CeO_2–ZrO_2–MO_x solid solution material having oxide anion conducting property as the promoter of CO oxidizing catalyst to fabricate the catalytic combustion-type CO gas sensor which can operate at considerably lower temperatures where other gases do not interfere the CO detecting performance.

Chapter 1

A novel catalytic combustion-type carbon monoxide gas sensor was devised by employing a 10 wt% Pt/$Ce_{0.68}Zr_{0.17}Sn_{0.15}O_{2.0}$ or 10 wt% Pt/$Ce_{0.76}Zr_{0.19}Zn_{0.05}O_{1.95}$ solids as the CO oxidizing catalyst. Since these catalysts can completely oxidize CO below 65 °C, the sensors incorporating these catalysts exhibited superior performance for the CO detection at 70 °C which is substantially lower than that (ca. 400 °C) required for the operation of the sensors with the conventional CO oxidation catalyst of Pt/Al_2O_3 or Pd/Al_2O_3. Although both sensors with 10 wt% Pt/$Ce_{0.68}Zr_{0.17}Sn_{0.15}O_{2.0}$ or 10 wt% Pt/$Ce_{0.76}Zr_{0.19}Zn_{0.05}O_{1.95}$ solids showed reliable sensing performance of quantitative and continuous response to CO gas concentration change, the sensor with 10 wt% Pt/$Ce_{0.68}Zr_{0.17}Sn_{0.15}O_{2.0}$ catalyst possess slightly rapid response.

Chapter 2

The response time of the catalytic combustion-type CO gas sensor with 10 wt% Pt/$Ce_{0.68}Zr_{0.17}Sn_{0.15}O_{2.0}$ catalyst as the CO oxidizing catalyst was able to shorten by insertion of aluminum nitride (AlN) as an intermediate heat transfer layer between the Pt coil and the CO oxidizing catalyst. Due to the high thermal conductivity of AlN, the combustion heat generated on the catalyst smoothly conducted to the Pt coil, resulting in rapid temperature change of Pt and

subsequently the resistance change of Pt. In addition, rapid heat transfer through AlN layer also results in the improvement of sensitivity, which might be by large amount of heat conduction to Pt coil.

Chapter 3

A catalytic combustion-type CO gas sensor was devised by using the precious metal-free CO oxidizing catalyst of 15.9 wt% $La_{0.87}Co_{1.13}O_3$-loaded $Ce_{0.67}Zr_{0.18}Sn_{0.15}O_{2.0}$. Since the 15.9 wt% $La_{0.87}Co_{1.13}O_3/Ce_{0.67}Zr_{0.18}Sn_{0.15}O_{2.0}$ catalyst oxidized CO completely at 130 °C, the sensor with 15.9 wt% $La_{0.87}Co_{1.13}O_3/Ce_{0.67}Zr_{0.18}Sn_{0.15}O_{2.0}$ catalyst showed smooth and reproducible response to CO gas at ca. 130 °C. Moreover, the sensor exhibited a linear relationship between sensor signal and CO gas concentration with rapid 50% response time of 20–40 s, similar to the case for precious metal containing catalyst of 10 wt% $Pt/Ce_{0.68}Zr_{0.17}Sn_{0.15}O_{2.0}$.

References

1) N. Taguchi, "Gas detection semiconductor element." *Japanese patent application,* 1962, S45-38200.

2) W. Göpel, K.D. Schierbaum, *Sens. Actuators B,* 1995, **26**, 1.

3) H. Yamaura, Hiroyuki, *J. Electrochem. Soc*., 1996, **143**, L36.

4) M. Gaidi, B. Chenevier, and M. Labeau, *Sens. Actuators B,* 2000, **62**, 43.

5) G. Korotcenkov, *Sens. Actuators B,* 2007, **121**, 664.

6) B. Bahrami, A. Khodadadi, M. Kazemeini, and Y. Mortazavi, *Sens. Actuators B,* 2008, **133**, 352.

7) K.F.Blurton, J.R. Stetter, *J. Chrom*., 1978, **155**, 35.

8) A. Yasuda, N. Yamaga, K. Doi, T. Fujioka, and S. Kusanagi, *Solid State Ionics*, 1990, **40–41**, 476.

9) S.A. Waghuley, S.M. Yenorkar, and S.S. Yawale, *Sens. Actuators B,* 2007, **125**, 921.

10) J. R. Stetter and J. Li, *Chem. Rev*., 2008, **108**, 352.

11) J. Eric and R. P. Townsend. "Combustible gas detectors." *U.S. Patent No. 4*, 1978, 123,225..

12) T. Ozawa, Y. Ishiguro, K. Toyoda, M. Nishimura, T. Sasahara, T. Doi, *Sens. Actuators B,* 2005, **108**, 473.

13) M.Sakaguchi, A.Ishikawa, I.Hoshihara, *J. Comb Soc. Jpn*., 2009, **51**, 129.

14) M. Ghasdi, H. Alamdari, *Sens. Actuators B,* 2010, **148**, 478.

15) Yasuda, A. Yoshimura, A. Katsuma, T. Masui, N. Imanaka, *Bull. Chem. Soc. Jpn.*, 2012, **85**, 522.

16) M.Y. Kim, T. Kamata, T. Masui, and N. Imanaka, *J. Mater. Sci. Res*., 2013, **2**, 51.

17) M. Y. Kim, T. Kamata, T. Masui and N. Imanaka, *Catalysts*, 2013, **3**, 646.

18) T. Masui, T. Kamata, N. Fukuhara, and N. Imanaka, *Bull. Chem. Soc. Jpn*., 2015, **88**, 746.

19) T. B. Nguyen, J. P. Deloume, V. Perrichon, *Appl. Catal. A: Gen*., 2003, **249**, 273.

20) Y. -Z. Chen, B. -J. Liaw, C. -W. Huang, *Appl. Catal. A: Gen*., 2006, **302**, 168.

21) T. Baidya, A. Gupta, P. A. Deshpandey, G. Madras, M. S. Hegde, *J. Phys. Chem. C*, 2009, **113**, 4059.

22) R. D. Shannon, *Acta Cryst*., 1976, **A32**, 751.

23) X.Yan, Q. Huang, B. Li, X. Xu, Y. Chen, S. Zhu, and S. Shen, *J. Ind. Eng. Chem.*, 2013, **19**, 562.

24) L. H. Ahrens, *Geochem. Cosmochem. Acta*, 1952, **2**, 155.

Acknowledgements

The author would like to express her heartfelt gratitude to Professor Dr. Nobuhito Imanaka, Department of Applied Chemistry, Graduate School of Engineering, Osaka University, for his continuous guidance, many invaluable suggestions, and his science encouragement throughout the work. The author is indebted to Professor Dr. Shinji Tamura, Department of Applied Chemistry, Graduate School of Engineering, Osaka University, for his continuous guidance and stimulating discussions for carrying out this work. The author is also very grateful to Dr. Naoyoshi Nunotani, Department of Applied Chemistry, Graduate School of Engineering, Osaka University, for his helpful suggestions and apposite advice.

The author is deeply grateful to Professor Dr. Susumu Kuwabata and Professor Dr. Ken-ichi Machida, Department of Applied Chemistry, Graduate School of Engineering, Osaka University, for reviewing this thesis and giving their valuable comments.

Special thanks should be given to author's seniors and co-workers, Dr. Yasuhisa Uneme, Mr. Syun Yasuhara, Mr. Masayoshi Umeda, Ms. Yuka Watanabe, Mr. Muhammad Radzi Iqbal, Mr. Rodlamul Pattaraphon, Ms. Haruka Nakatani, for their helpful assistance and support in the course of this work, and the other members of the research group under direction of Professor Dr. Nobuhito Imanaka, Osaka University.

The Japan Society for the Promotion of Science is also acknowledged for a research fellowship.

Finally, the author would like to extend deep gratitude to her parents, Mr. Masahiro Hosoya and Ms. Akemi Hosoya, her younger brother, Mr. Daiki Hosoya, her younger sisters, Misa Hosoya and Haruna Hosoya, and all members of her family for their encouragement, continuous understanding, and perpetual supports.